Available online at www.sciencedirect.com
SCIENCE DIRECT®
Journal of Chromatography A, 1008 (2003) 193–203
JOURNAL OF CHROMATOGRAPHY A
www.elsevier.com/locate/chroma

Dynamics of gel isoelectric focusing with ampholytic dyes monitored by camera in real-time

Miroslava Štastná*, Karel Šlais
Institute of Analytical Chemistry, Academy of Sciences of the Czech Republic, Veveri 97, 611 42 Brno, Czech Republic

Received 5 March 2003; received in revised form 28 April 2003; accepted 27 May 2003

Abstract

The dynamics of gel isoelectric focusing were studied by using amphoteric low-molecular-mass colored substances (isoelectric point markers). The polyacrylamide gel in slab format was in direct contact with the electrodes. In addition to isoelectric focusing with a pH gradient composed of synthetic carrier ampholytes, pH gradients created by simple buffers of acetic acid, 2-(*N*-morpholino)ethanesulfonic acid, histidine and *N*,*N*,*N*′,*N*′-tetramethylethylenediamine were applied. The progress of the electrofocusing process was monitored by a charge-coupled device camera and video recording. The gradient profile and dynamics were approximated from the positions of isoelectric point markers, which were focused both on boundaries between individual zones of simple buffers and within the zones themselves. The obtained animated records enabled the observation of the entire real focusing run within fractions of a minute, which is useful both for the understanding and optimization of the focusing.

Keywords: Isoelectric focussing; Polyacrylamide gels; Isoelectric point markers; Video monitoring; Detection, electrophoresis; Dyes

1. Introduction

Isoelectric focusing (IEF) is an electrophoretic technique in which amphoteric substances are separated on the basis of differences in their isoelectric points in an electric field. The isoelectric point (p*I*) of a substance is defined as the pH at which the amphoteric substance displays no net charge. IEF has been a powerful analytical separation method since 1961 when the first paper published by Svensson [1] appeared. In the very first years of IEF, the pH gradient as a result of the electrolysis of a simple salt was created and the zone of pure water separating anions of the salt from the cations was observed. To understand and ensure the proper IEF process, the observation and study of its dynamics are necessary with reference to pH gradient linearity and stability, IEF completion and instrumentation.

The aim of this study was to show a method for observing the dynamics of IEF in real-time using present-day tools. To efficiently demonstrate the dynamics of IEF, we considered several points: (i) formation of a pH gradient created by the simplest compositions of simple electrolytes as well as the linear gradient created by synthetic carrier am-

*Corresponding author. Fax: +420-541212113.
E-mail address: stastna@iach.cz (M. Štastná).

0021-9673/03/$ – see front matter
doi:10.1016/S0021-9673(03)00968-3

pholytes; (ii) approximation of pH values within the gradient by different colored and a broad pH range covering p*I* markers during the entire analysis run; and (iii) instrumentation suitable both for minimizing the pH gradient instability and for camera monitoring in real-time.

1.1. pH gradient background

In this work the dynamics were demonstrated in a pH gradient created by both synthetic carrier ampholytes and simple buffers. The simple buffers were previously used for the gradient modification [2–7] and allowed us to generate the pH gradient shapes including the plateau widths and edge heights in their changes with time. The simple electrolytes in a pH gradient background were chosen based on their presence in IEF gels [*N*,*N*,*N*′,*N*′-tetramethylethylenediamine (TEMED)—weak base, K_2SO_4—strong electrolyte], or as examples of well-known buffers [acetate—weak acid, histidine—good ampholyte, 2-(*N*-morpholino)ethanesulfonic acid (MES)—poor ampholyte].

1.2. Approximation of pH across the entire gel plate

At present, only a few naturally colored proteins are available and used as standards in IEF. The employment of new synthetic UV-detectable peptide p*I* markers [8,9] or fluorescence-labeled peptide p*I* markers [10,11] in capillary IEF was published recently. To study the evolution of pH gradient in time, laborious procedures were applied in which the gel was sectioned into pieces, gel slices extracted and the pH measured on each slice [12] or later the device for automated pH measurement was employed [13]. The other attempt to monitor the pH gradient shape was carried out by using the natural fluorescence of the carrier ampholytes in synthetic carrier ampholyte mixtures, which allowed the monitoring and visualization of the pH gradient evolution in real-time [14]. To visualize the positions of colorless proteins in time, a set of IEF gels had to be run, stained and photographed in gradual electrofocusing time, although the reproducibility of such gels could be disputed. In addition, in case of protein labeling, the intensity of the colored products obtained by using visible color dyes is largely insufficient for applications with thin gel slabs and real time monitoring; the color range and heterogeneity for both fluorescent and visible color labeled proteins is also a limitation. Compared to the color labeled protein markers, the p*I* markers previously described as aminomethylated nitrophenols [15] and sulfonephthaleins [16] as well as compounds of a similar nature and newly developed in our group possess high color intensity at a relatively low concentration, various color spectrums, p*I* values over a wide range, good solubility and no precipitation in boundaries of pH gradient background. Even in very thin gel layers, they allowed us to reach the band color intensity sufficient for convenient observation by the naked eye or by camera for video documentation purposes. Since the p*I* markers used have their titration curves mutually different as well as different from pH gradient background components, the pH of their environment need not correspond precisely to the marker p*I* value during pH gradient changes. Nevertheless, their positions can indicate the end of the pH gradient formation as well as the speed of pH gradient decay.

1.3. Instrumentation ensuring the stable pH gradient and monitoring in real-time

Two phenomena connected with the stability of the pH gradient known as gradient drift and the ‘‘plateau’’ effect took place when a longer time for separation was needed [17,18]. To prevent the migration of gradient components out of the separation chamber into the electrolyte reservoirs, the suggestions were made, to isolate the focusing space from the electrolyte chambers using ion-exchange membranes or to choose the optimum concentration and composition of analyte/catholyte, which would keep the gradient components of interest within the focusing space [19,20]. A comparison of different electrode assemblies referring to the nature and relative volume of the electrode electrolytes and the types of membranes used to isolate those electrolytes from the separation space was done in a capillary system [21]. In 1990 the differential equations were given for a more accurate calculation of pH gradients generated by weak acids/bases [22]. The other possible way to solve the problem of the pH gradient

instability was to use immobilized pH gradients [23–25]. The dynamics of IEF and the influence of the IEF apparatus on the stability of the pH gradient were also studied by using computer simulations. The most effective approach is to keep the volume of the reservoir small with respect to that of the focusing space to minimize gradient drift [18] or the electrode electrolytes are avoided for short gels [26]. The instrumentation for real-time and whole column imaging detection was described for IEF performed in capillary format [27]. In our study, the experimental arrangement without electrode electrolyte reservoirs was used. In order to minimize the diffusion of gradient components into the space behind the electrodes and thus to ensure the stability of the pH gradient with time, the space behind the electrodes was minimized by reduction of the original gel size. The cell for gel running was chosen and modified in order to insert it into the darkroom of the documentation system (described in detail in Section 2.3) equipped with a charged-coupled device (CCD) camera and to document the gradient formation in real-time.

2. Experimental

2.1. Materials

All chemicals used were of analytical-reagent grade. Acrylamide was purchased from Serva (Heidelberg, Germany); *N*,*N*′-methylene-bis-acrylamide (Bis), ammonium persulfate, TEMED and MES were from Merck (Darmstadt, Germany). Glycerol was obtained from Onex (Roznov pod Radhostem, Czech Republic), K_2SO_4 from Lachema (Brno, Czech Republic), L-Histidine from Aldrich (designated as His, Steinheim, Germany) and synthetic carrier ampholytes Bio-Lyte 3/10 Ampholyte, 40% solution from Bio-Rad Labs (Hercules, CA, USA). The previously described aminomethylated nitrophenols [15] and sulfonephthaleins [16] as well as compounds of a similar nature newly developing in our group were used as colored good ampholytes for the indication of the local pH in pH gradient. The isoelectric points of the latter ones were determined and calculated by comparison to both the protein standards commercially available (Merck) and the anthranilic acids [28].

2.2. Polyacrylamide gels

The polymerization procedure used was as follows. Acrylamide-Bis stock solution (25% T, 3% C)[1] was prepared, filtered through a 0.45-μm filter (Millipore, MA, USA) and stored at 4 °C in the dark. The polymerization mixture of five-times diluted acrylamide-Bis stock solution (the final gel composition 5% T, 3% C), 5% (w/v) glycerol and Bio-Lyte 3/10 ampholyte (final concentration from 0.5 to 3%) was degassed in an ultrasonic bath for 5 min. Then two initiators, 5 μl of TEMED and 25 μl of 10% (w/v) ammonium persulfate per 5 ml of degassed solution were added and swirled gently. Polymerization mixture with initiators was pipetted between the glass plate and the casting tray (Bio-Rad Labs). In order to minimize diffusion of gradient components into the space behind the electrodes [22], the original gel size (125×65×0.4 mm) was reduced to the size of 125×54×0.4 mm. After polymerization was complete, the gel on the casting tray was stored overnight at 4 °C, and wrapped in plastic foil to prevent the surface of the gel from drying out.

In other sets of experiments, acetic acid, acetic acid and MES, acetic acid and His or acetic acid and K_2SO_4, were added to the polymerized gel instead of Bio-Lyte 3/10 ampholytes.

2.3. Equipment

A model 111 Mini IEF Cell (Bio-Rad Labs) was used for running the gels. A schematic representation of the running chamber is shown in Fig. 1. In brief, the samples between 0.5 and 2 μl were loaded onto the gel (5) supported by a glass plate (4) by means of a template provided by the manufacturer. After diffusion of the samples into the gel (ca. 5 min), the gel was turned upside-down and placed directly on the two graphite electrodes (3) in the running chamber (1). Before analysis the transparent lid connected with power cables (not shown) was slid

[1] T=(g acrylamide+g bis)/100 ml solution; C=g bis/% T.

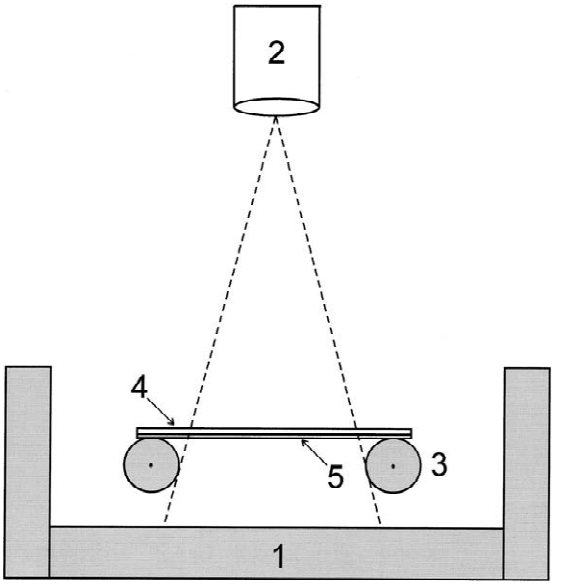

Fig. 1. Schematic representation of IEF cell. (1) Outer chamber; (2) CCD camera; (3) graphite electrodes, 50-mm distance between contact points; (4) glass plate; (5) polyacrylamide gel of size 125×54×0.4 mm.

into the top of the chamber and placed in the darkroom of The Gel Doc 2000 Gel Documentation System (Bio-Rad Labs) equipped by CCD camera (2) and epi-white light illumination allowing us to obtain the images in real-time. The CCD camera was supplied as an integral part of The Gel Doc 2000 Gel Documentation System. The power supply VNZ 22 (Czech Republic) was used for running at constant electric power of 0.6 W. To obtain the color image and to document the bands, which are in the shadows of the round electrodes and cannot be seen during the CCD camera scanning, after the focusing run, the glass plate with the gel was removed carefully from the electrodes and scanned by a UMAX Astra 3400 scanner (UMAX Technologies, Dallas, TX, USA).

2.4. Data processing

The gel images in epi-white light illumination were scanned in real time by means of Scion Image for Windows software (Scion, USA) in 3-min intervals (40 scans during 2 h). The position of the band of interest in the gel was characterized by the R_f value, which was evaluated by means of Quantity One Software, Version 4.2.3 (Bio-Rad Labs). Here, R_f is defined as the ratio between distance of band from anode to total distance of both electrodes. The color images were processed by use of Adobe PhotoDeluxe Home Edition 3.0 software (Adobe Systems, USA).

3. Results and discussion

3.1. IEF with synthetic carrier ampholytes

The example of time course of IEF with 3% (v/v) Bio-Lyte 3/10 ampholyte in polyacrylamide gel (5% T, 3% C) is shown in the montage in Fig. 2. The p*I* markers were electrofocused in a wide-range pH gradient created by synthetic carrier ampholytes having a working pH range of 3.5–9.5 (provided by the manufacturer). The IEF was completed in approximately in 1 h and the gel pattern did not change significantly after scan 17. The bands remained focused and stable in the proper positions of pH gradient for an additional 1 h or more (not shown) with no drift observed. This could be explained by experimental arrangement in which the running gel is placed directly on the round electrodes with minimized electrode space and without any electrode buffer reservoirs. In this arrangement the electrodes create the fixed end of the gel and bands do not drift out of the gel over a prolonged time (see theory) [18,22].

In Fig. 3 the gel image is presented after the IEF analysis was finished and the gel was scanned by UMAX scanner. The bands that were positioned close to the electrodes and could not be seen by CCD camera were scanned at both anodic (lanes 1, 2, 4; white spots) and cathodic (lanes 1, 3, 5) ends of the gel. Their stable positions demonstrate the stability of the ends of the pH gradient during prolonged analysis times. In Fig. 3, a black and white record converted from a color image is presented. Unfortunately, the time delay between the last CCD camera scan and UMAX scan causes broader zones in the latter due to diffusivity of low-molecular-mass colored p*I* markers. The color images that better reflect the situation and illustrate the colors of p*I* markers can be found at http://www.iach.cz/liq

The linearity of the pH gradient across the gel was

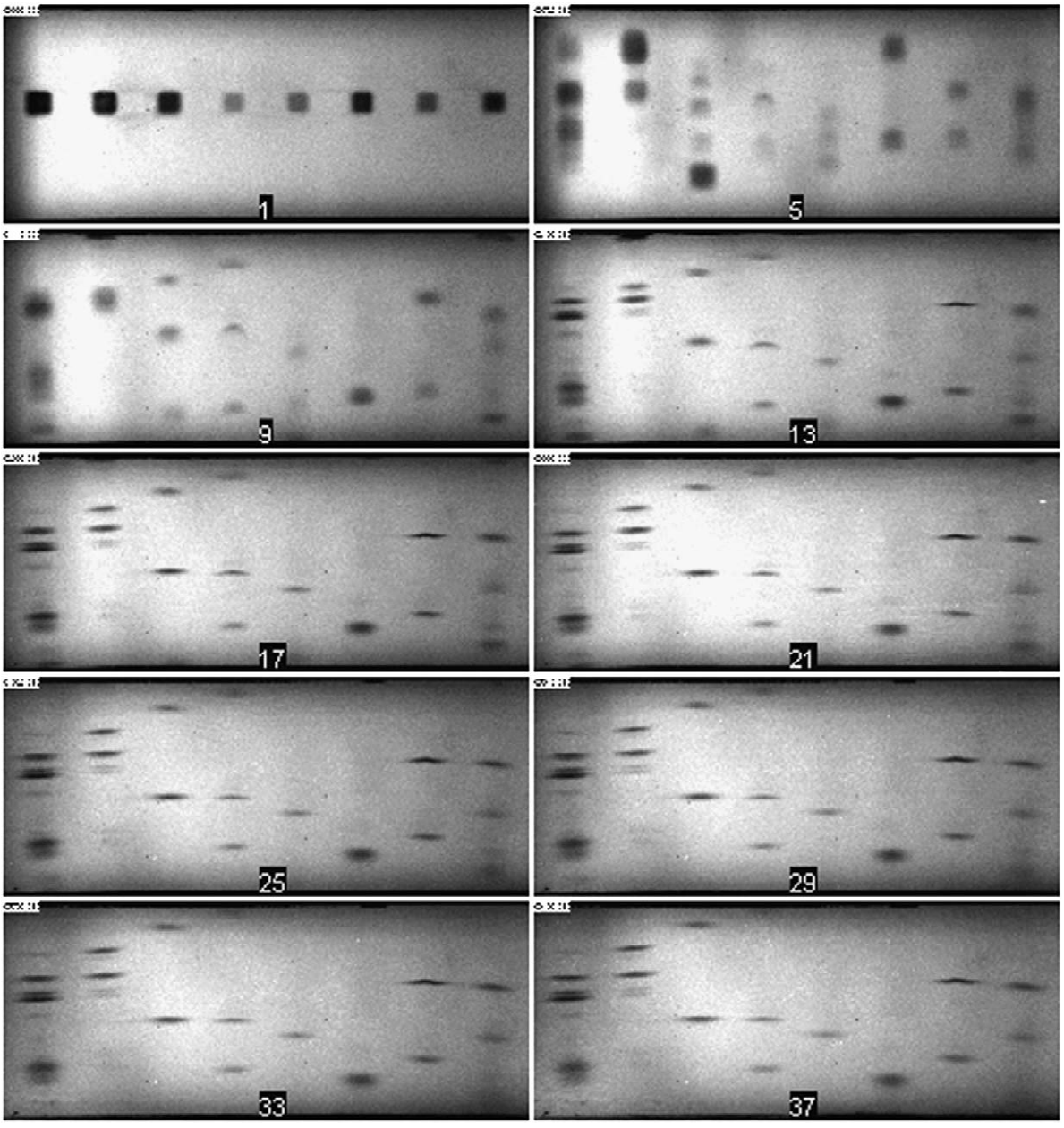

Fig. 2. Montage representing the evolution of electrofocusing of p*I* markers on the background of synthetic carrier ampholytes 3% (v/v) Bio-Lyte 3/10 in polyacrylamide gel (5% T, 3% C). The mixtures of p*I* markers were loaded into eight lanes in the middle of the gel. A constant electric power of 0.6 W was applied. The voltage increased from 75 to 400 V simultaneously as the electric current decreased from 7.7 to 1.5 mA. The gel was monitored in 3-min intervals during 2 h (40 scans in total). Numbers at the middle bottom of each gel mark the scan number. The acidic end of the pH gradient is at the top and the basic end at the bottom of the gel.

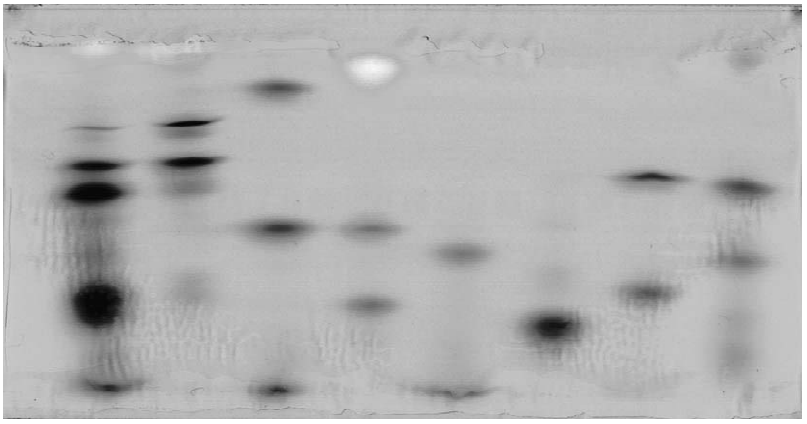

Fig. 3. Gel image obtained by transferring the gel from IEF cell on the UMAX scanner after electrofocusing was completed. For experimental conditions see Fig. 2.

tested by using isoelectric points and R_f values of p*I* markers and the resulting plot is shown in Fig. 4A. The pH gradient can be considered sufficiently linear with some non-linearity in the vicinity of the electrodes.

The stability of band positions and thus the stability of pH gradient with time after proper isoelectric points are reached can be seen in Fig. 4B for several p*I* markers chosen. It is also interesting that two p*I* markers (isoelectric points 8.39 and 8.80) have inverse positions in the gel around scan 12. Our explanation of this phenomena lies in differences of dz/dpH values of both p*I* markers. The p*I* marker with an isoelectric point of 8.39 has a substantially higher dz/dpH value compared to the p*I* marker with an isoelectric point of 8.80 and it copies the pH gradient during its creation more exactly than the p*I* marker with lower dz/dpH value. Thus it could be possible that before the pH gradient across the gel is established, the p*I* marker with a higher dz/dpH value can run over its p*I* value in pH gradient, and after the stable pH gradient is formed this p*I* marker returns back to its proper position. This movement forward and backward in the gel was also visually observed during the IEF run simultaneously with the shape of the bands reflecting the different values of dz/dpH and will soon be available in the form of the animation at the Web address mentioned above.

3.2. IEF in simple buffers

It was shown that the steady state in IEF can also be reached when the simple buffers instead of carrier ampholytes were used. This was mathematically described and demonstrated in the density gradient column arrangement [4,22]. In the gel IEF where the presence of TEMED is necessary for polymerizing acrylamide, the corrections for TEMED in steady state calculations were included [18,29]. In order to visualize the dynamics of electrofocusing in simple buffers, the simplest electrolyte compositions were examined as follows. The simple electrolytes in pH gradient background were chosen based on their presence in IEF gels (TEMED—weak base, K_2SO_4—strong electrolyte), or as examples of well-known buffers (acetate—weak acid, histidine—good ampholyte, MES—poor ampholyte) [18].

3.2.1. Electrofocusing in acetic acid-TEMED system

In the next experiments only acetic acid with no synthetic carrier ampholytes was added before the gel polymerization. The total concentration of the acetic acid in the gel was 8.5 m*M* in order to neutralize the 8.5 m*M* concentration of TEMED inevitably used as a initiator in polymerization process. A constant electric power of 0.6 W was set at the beginning of each analysis with the voltage limit varying from 800 down to 50 V. After the voltage limit was reached the analyses continued in the constant voltage mode. The typical gel pattern observed with the 100 V limitation is shown in Fig. 5 and R_f vs. time (scan number) plots for voltage

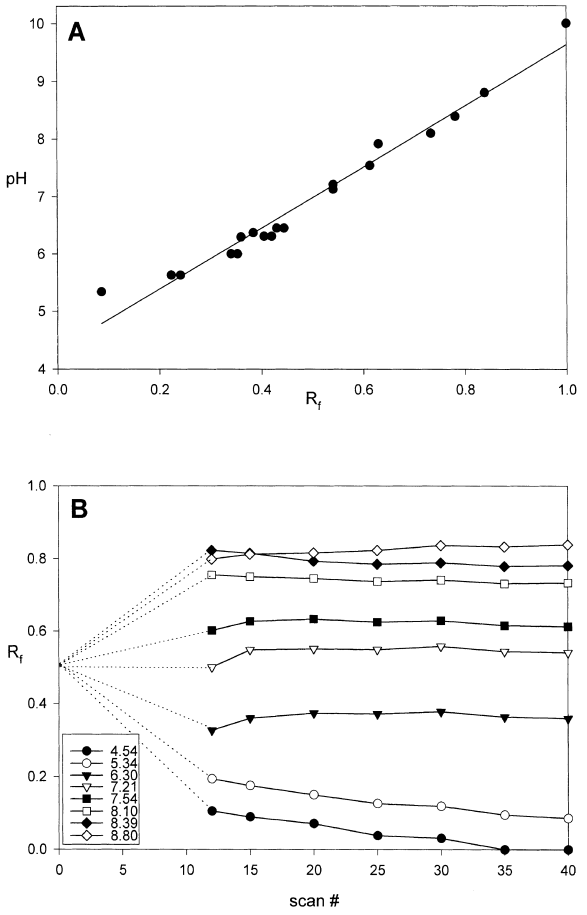

Fig. 4. (A) Test of linearity of pH gradient created by synthetic carrier ampholytes across the gel. (B) Example of the stability of pH gradient with time for a few p*I* markers chosen. Experimental conditions as in Fig. 2.

limits of 50, 100, 200 and 800 V are presented in Fig. 6A–D, respectively. The p*I* markers used in the experiment marked the boundaries between zones of TEMED, water, acetic acid and H_2SO_4, respectively, created during electrofocusing. The pH range in the edges between zones of simple electrolytes can be approximated by means of values of the isoelectric points included as depicted in the inset of Fig. 6A. The sulfate anion, which originated from ammonium persulfate initiator, was concentrated at the H_2SO_4 zone in the vicinity of the anode. It was separated from the zone of acetic acid by a boundary visualized by the p*I* marker with an isoelectric point value of 2.49. The p*I* markers having their p*I* values above this value were separated in the zone of acetic acid (the zones were slightly yellow and thus were not seen in a black and white image). The boundary between zones of acetic acid and water was approximated by several p*I* markers with isoelectric points covering the range from 3.70 to 4.65. The zone of water that was created in all experiments widened with increases in voltage. Another boundary positioned between the zones of water and TEMED was visualized by p*I* markers with isoelectric points in the range 5.34–7.54. The p*I* markers with p*I* values above 7.54 were separated within the zone of TEMED up to a pH equal to 10.00, which was given by p*I* markers sitting at the cathode. Ammonium ion originated from ammonium persulfate has a p*K* value equal to 9.25, which is similar to the p*K* value of TEMED, and can be expected to be incorporated within the TEMED zone. The dotted lines in Fig. 6 express the imaginary progress of analysis between sampling position in the middle of the gel (R_f=0.5) and the position of p*I* markers in which their bands were first in focused form. The white spots of the gel in Fig. 5 belong to the yellow colored p*I* markers while the gray and black bands correspond to p*I* markers colored from orange to red or violet.

An example of the three-dimensional plot of pH vs. R_f vs. scan number is shown in Fig. 7 for p*I* markers with isoelectric points mentioned above with the voltage limitation up to 800 V.

3.2.2. Electrofocusing in acetic acid–MES–TEMED system

In order to visualize the zone of ampholytic buffer, MES and His were used as components of the pH gradient background.

When MES in addition to acetic acid and TEMED was added to the gel before polymerization, a new zone of MES was created between zones of acetic acid and water. As illustrated in Fig. 8A, as the concentration of MES increases and its zone becomes wider simultaneously with the zone of acetic acid, the zones of both water and TEMED had the opposite trend. For evaluation, the last scans for each MES concentration were taken. The p*I* values of p*I* markers positioned in boundaries are given in the inset of Fig. 8B. The other p*I* markers applied were separated within zones of acetic acid, MES and TEMED, respectively (e.g. p*I* markers with p*I* values of 3.85, 3.90 and 8.80, respectively; Fig. 8).

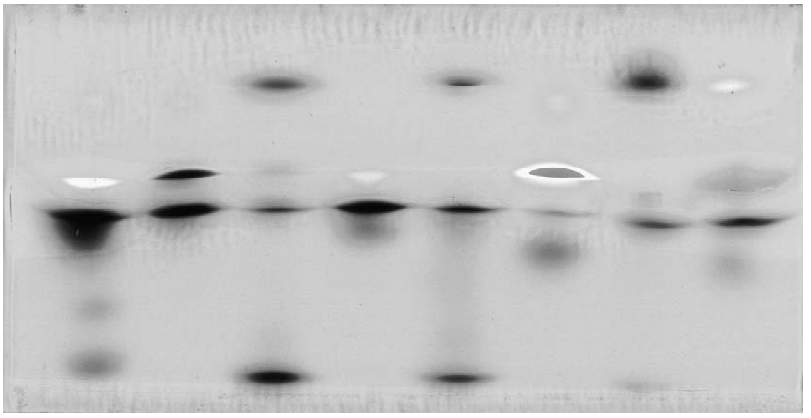

Fig. 5. Gel record representing the electrofocusing of p*I* markers in the acetic acid–TEMED system. The p*I* markers are focused both in boundaries and within the zones of acetic acid and TEMED. The three black (lanes 3, 5 and 7) and one white (in reality yellow; lane 8) bands at the top of the gel mark the boundaries between the zones of H_2SO_4 close to the anode and acetic acid. Two visible boundaries, around the middle of the gel, confine the zone of water and restrict it from the zones of acetic acid and TEMED positioned at the lower part of the gel. The two black bands at the bottom of the gel (lanes 3 and 5) were focused in the vicinity of the cathode and with a prolonged analysis time did not change. The grey bands in the TEMED zone correspond to the p*I* markers that were more or less focused. The other p*I* markers focused in the zone of acetic acid are invisible in the figure presented due to only slightly yellow colors.

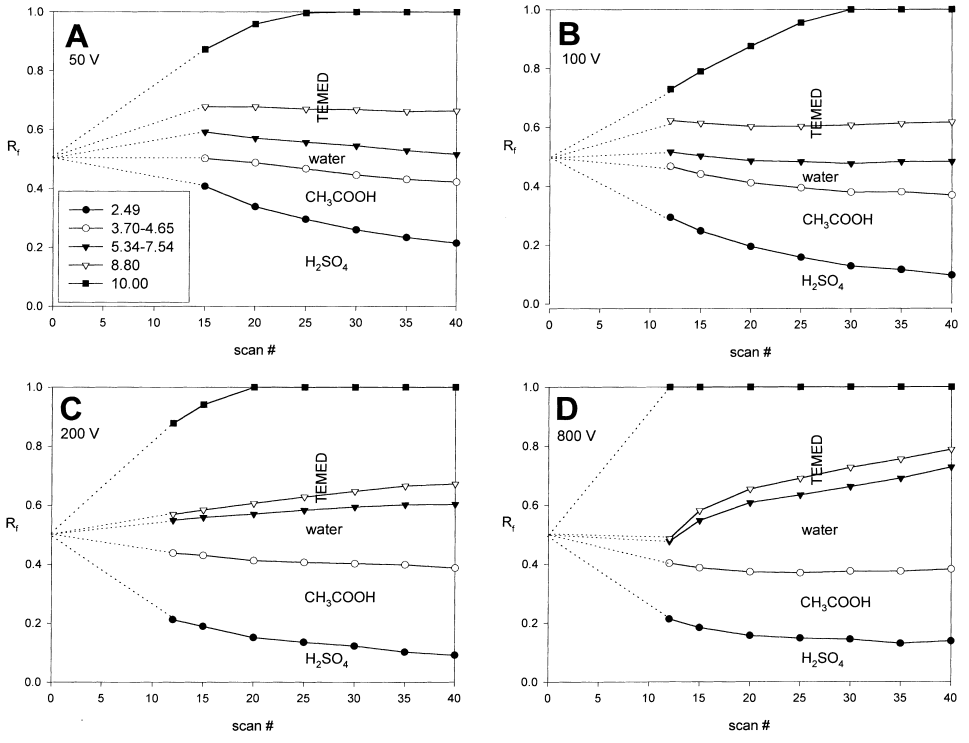

Fig. 6. Development of the individual background zones and their stability with time in the acetic acid–TEMED system. Initial experimental conditions at constant electric power of 0.6 W following by mode with constant voltage. Voltage limit: (A) 50 V, (B) 100 V, (C) 200 V, (D) 800 V. Other experimental conditions as in Fig. 5.

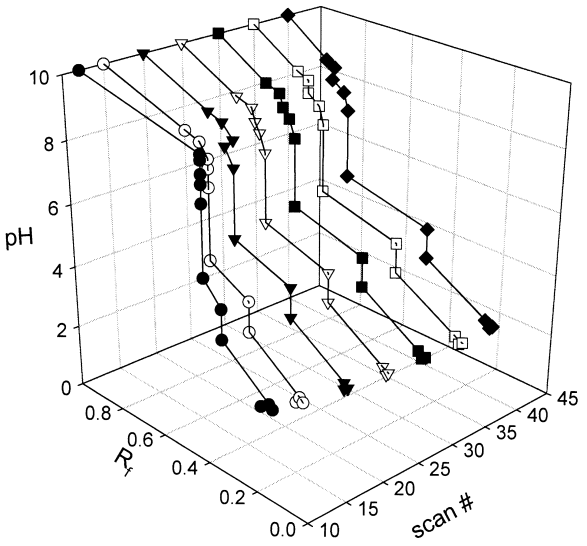

Fig. 7. Example of three-dimensional plot for electrofocusing in the acetic acid–TEMED system at voltage limitation up to 800 V. For experimental conditions, see Fig. 5.

3.2.3. Electrofocusing in acetic acid–His–TEMED system

Using His instead of MES in the system described in Section 3.2.2, the zone of His was created between zones of water and TEMED. This situation is illustrated in a graph in Fig. 9. The zone of water was confined by the boundaries marked by p*I* markers with p*I* values in the range 3.70–4.65 on one side and in the range 6.30–7.03 on the other side. The zone of His was separated from the TEMED zone by markers having a p*I* value of 8.80. Similarly, as in the acetic acid–MES–TEMED system, the other p*I* markers used were separated within the zones of acetic acid, His and TEMED, respectively, according to their isoelectric points. As can be seen from Fig. 9, the p*I* markers with p*I* values of 5.63 and 6.00 were separated in a zone designed as a water zone. The following explanation could be given. The p*K* value of acetic acid stated in the literature is 4.76, the pK_2 value of MES is given as 6.10 and the p*I* of His is calculated as 7.59 (pK_2 and pK_3 values for His are 6.00 and 9.17, respectively). The difference between the p*K* value of acetic acid and p*I* value of His is then equal to 2.83. It could be possible that the zones of acetic acid and His do not have the sharp boundaries and are partly presented in the zone of water. Then the separation could occur in such a mixed zone. In contrast to the system mentioned in Section 3.2.2, where no separation was presented in the zone of water, the explanation should be in the smaller difference (equal to 1.34) between the p*K* of acetic acid and pK_2 of MES.

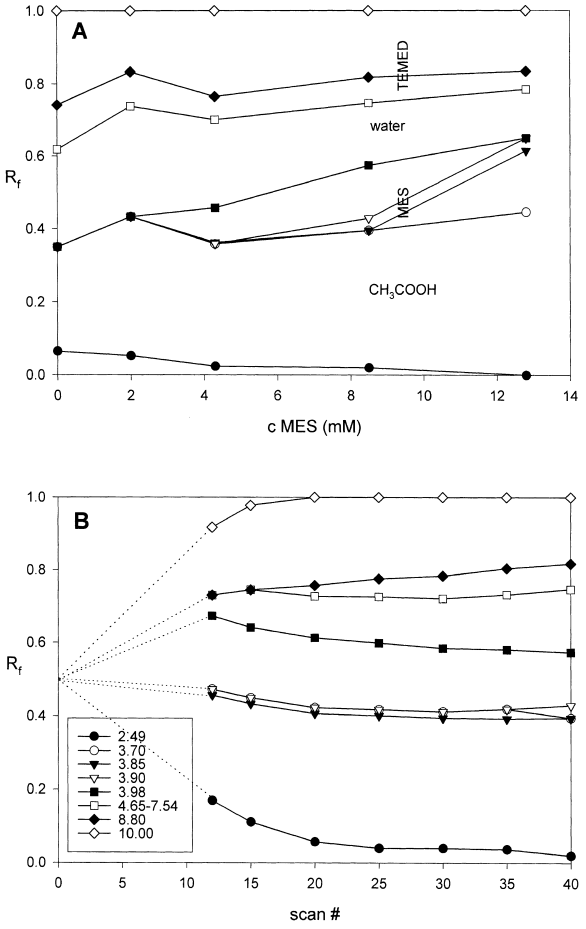

Fig. 8. Electrofocusing in acetic acid–MES–TEMED system. Final concentrations of acetic acid and TEMED in gel were kept the same as in Fig. 5 (8.5 m*M*). (A) Evolution of background zone boundaries with the increase in MES concentration. (B) Stability of the zones with time for 8.5 m*M* MES.

3.2.4. Electrofocusing with K_2SO_4

The sulfate ion is an inevitable component of a polyacrylamide gel since it comes from ammonium persulfate needed for gel preparation.

As expected, the increase in concentration of K_2SO_4 resulted in the narrowing of the zones of both

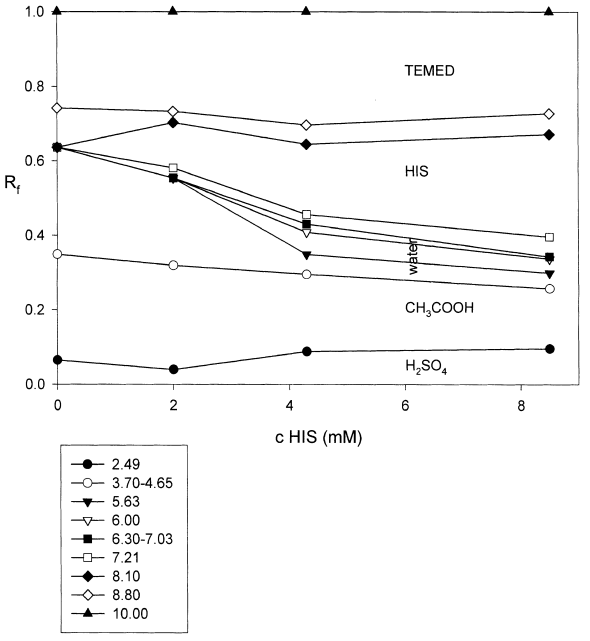

Fig. 9. Electrofocusing in acetic acid–His–TEMED system with varying His concentrations. Concentrations of acetic acid and TEMED in gel were kept constant at 8.5 m*M*.

acetic acid and water in the middle of the gel and in the broadening of the zones of H_2SO_4, TEMED and KOH at the sides of the gel (Fig. 10). The p*I*

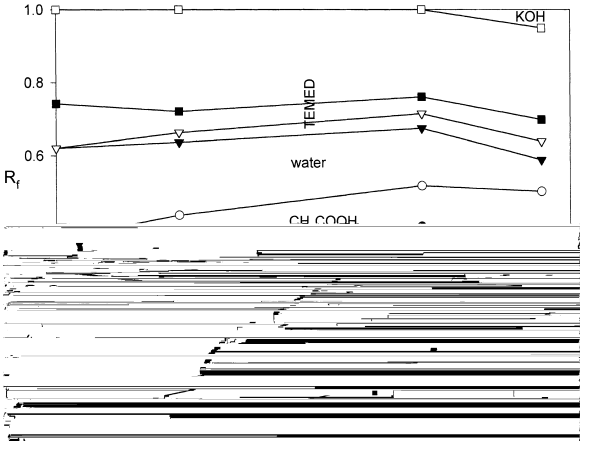

Fig. 10. Development of the boundaries in a system with increasing K_2SO_4 concentration. Concentrations of acetic acid and TEMED in gel were both 8.5 m*M*.

markers that did not lie in boundaries were focused within the zones of H_2SO_4, acetic acid and TEMED, respectively.

4. Conclusions

The on-line camera monitoring of gel plate is both close to the widely spread IEF mode and it also allows scanning of the whole separation path during the whole run time using currently available instrumentation. Furthermore, it enables us to observe several separation lanes and thus a large number of p*I* markers simultaneously so that a detailed course of the pH gradient can be obtained. In addition, the drop in electric current usually used for indication of the focusing completion is sometimes not quite explicit and then the indication by colored p*I* markers is much better. The approach used allowed us to conveniently approximate the pH gradient shape including the plateau widths and edge heights in their changes with time. Although the positions of p*I* markers need not indicate the exact pH values of their p*I* values, they enable us to indicate the end of focusing and gradient decay. By recording focusing runs in the gradients generated both from commercially available carrier ampholytes as well as from simple buffers, nearly stable pH gradients were obtained in the experimental arrangement used, which is in contrast to conventional IEF with electrode electrolyte reservoirs. The animated records also enabled the observation of the whole real focusing runs within a fraction of a minute, which is useful both for the understanding and for demonstration of the focusing. The approach used may be useful for design of IEF instrumentation, optimization of the electrofocusing time and modifying of the gradient shape.

Acknowledgements

Supported in part by grants from the Academy of Sciences of the Czech Republic (grant S4031201) and from the Grant Agency of the Czech Republic (grant 203/02/1447).

References

[1] H. Svensson, Acta Chem. Scand. 15 (1961) 325.
[2] N.Y. Nguyen, A. Chrambach, Anal. Biochem. 74 (1976) 145.
[3] R.A. Mosher, W. Thormann, R. Kuhn, H. Wagner, J. Chromatogr. 478 (1989) 39.
[4] E. Pettersson, Acta Chem. Scand. 23 (1969) 2631.
[5] J. Pospichal, E. Glovinova, J. Chromatogr. A 918 (2001) 195.
[6] T. Hirokawa, J. Chromatogr. A 686 (1994) 158.
[7] G. Weber, P. Bocek, Electrophoresis 19 (1998) 1649.
[8] K. Shimura, Z. Wang, H. Matsumoto, K. Kasai, Electrophoresis 21 (2000) 603.
[9] Y. Jin, G. Luo, T. Oka, T. Manabe, Electrophoresis 23 (2002) 3385.
[10] K. Shimura, K. Kasai, Electrophoresis 16 (1995) 1479.
[11] K. Shimura, K. Kamiya, H. Matsumoto, K. Kasai, Anal. Chem. 74 (2002) 1046.
[12] N.Y. Nguyen, A. Chrambach, Anal. Biochem. 73 (1976) 30.
[13] B.E. Chidakel, N.Y. Nguyen, A. Chrambach, Anal. Biochem. 77 (1977) 216.
[14] E. Gombocz, E. Cortez, Electrophoresis 20 (1999) 1365.
[15] K. Slais, Z. Friedl, J. Chromatogr. A 661 (1994) 249.
[16] K. Slais, Z. Friedl, J. Chromatogr. A 695 (1995) 113.
[17] P.G. Righetti, J.W. Drysdale, Ann. NY Acad. Sci. 209 (1973) 163.
[18] R.A. Mosher, D.A. Saville, W. Thormann, in: The Dynamics of Electrophoresis, VCH, Weinheim, 1992, p. 163.
[19] N.Y. Nguyen, A. Chrambach, Anal. Biochem. 79 (1977) 462.
[20] N.Y. Nguyen, A. Chrambach, Anal. Biochem. 82 (1977) 54.
[21] R.A. Mosher, W. Thormann, M. Bier, J. Chromatogr. 436 (1988) 191.
[22] R. Hagedorn, G. Fuhr, Electrophoresis 11 (1990) 281.
[23] B. Bjellqvist, K. Ek, P.G. Righetti, E. Gianazza, A. Gorg, W. Postel et al., J. Biochem. Biophys. Methods 6 (1982) 317.
[24] P.G. Righetti, E. Gianazza, Electrophoresis 13 (1992) 185.
[25] P.G. Righetti, C. Tonani, in: F. Dondi, G. Guiochon (Eds.), Theoretical Advancement in Chromatography and Related Separation Techniques, Kluwer, Dordrecht, 1992, p. 581.
[26] R. Westermeier, in: Electrophoresis in Practice, VCH, Weinheim, 1993, p. 43.
[27] X.H. Fang, C. Tragas, J.Q. Wu, Q.L. Mao, J. Pawliszyn, Electrophoresis 19 (1998) 2290.
[28] P. Leggate, G.E. Dunn, Can. J. Chem. 43 (1965) 1158.
[29] P.J. Svendsen, C. Schafer-Nielsen, in: Electrophoresis'79, Walter de Gruyter and Co, New York, 1980, p. 265.